

Contents lists available at SciVerse ScienceDirect

Journal of Alloys and Compounds

journal homepage: www.elsevier.com/locate/jalcom



Hydrogen storage properties and thermal stability of amorphous $Mg_{70}(RE_{25}Ni_{75})_{30}$ alloys

He-xin Chen, Zhong-min Wang*, Huai-ying Zhou, Chen-yuan Ni, Jian-qiu Deng, Qing-rong Yao

School of Materials Science & Engineering, Guilin University of Electronic Technology, No. 1, Jinji Road, Guilin 541004, China

ARTICLE INFO

Article history: Received 21 December 2012 Received in revised form 21 January 2013 Accepted 21 January 2013 Available online 10 February 2013

Keywords: Mg alloy Amorphous alloys Hydrogen storage properties Thermal stability

ABSTRACT

In this study, amorphous $Mg_{70}(RE_{25}Ni_{75})_{30}$ (RE = La, Pr, Nd) alloys were produced by melt spinning, their hydrogen storage properties and the thermal stabilities have been studied by means of PCTPro2000 and Differential Scanning Calorimetry (DSC), respectively. After hydrogenation of $Mg_{70}(RE_{25}Ni_{75})_{30}$ samples at 573 K under 2 MPa hydrogen pressure, XRD results indicate the formation of new phases of MgH_2 , Mg_2NiH_4 , $LaH_{3.01}$ (RE = La), $PrH_{2.92}$ (RE = Pr) and Nd_2H_5 (RE = Nd). The experimental data of hydrogen desorption kinetics at 523 K, 553 K, 573 K are well fitted through Avrami–Erofeev equation, and the hydrogen desorption kinetics were in the order of Pr > La > Nd. Based on the results of DSC analysis, dehydrogenation activation energies of these samples were determined to be 68.81 ± 2.50 kJ/mol (RE = La), 64.79 ± 1.09 kJ/mol (RE = Pr) and 73.37 ± 3.23 kJ/mol (RE = Nd), which are in accordance with the results of hydrogen desorption kinetics. As shown in the P–C isotherm curves, two hydrogen absorption plateaus at about 0.07 MPa and 0.2 MPa have been observed for $Mg_{70}(RE_{25}Ni_{75})_{30}$ (RE = La, Pr) tested at 573 K, while there is only one sloping hydrogen absorption plateau in the range of 0.06-0.3 MPa for $Mg_{70}(Nd_{25}Ni_{75})_{30}$ alloy. The maximum hydrogen absorption capacity is 4.21 wt.% for $Mg_{70}(Nd_{25}Ni_{75})_{30}$ and the maximum hydrogen desorption capacity is 2.74 wt.% for $Mg_{70}(Nd_{25}Ni_{75})_{30}$.

© 2013 Elsevier B.V. All rights reserved.

1. Introduction

Hydrogen storage in metal hydrides is one of the most promising solutions to meet the requirements for mobile and stationary applications [1]. Magnesium and magnesium alloys are particularly attractive for the solid-state storage of hydrogen due to their high theoretical storage capacity of up to 7.6 wt.%-H (in the case of pure MgH₂), light weight and low cost [2]. However, the very slow hydrogen absorption/desorption kinetics and high hydrogen absorption/desorption temperature prevent them from many practical applications. Generally, the strategy for improving the hydrogen absorption/desorption kinetics of magnesium alloys can be divided into two categories. One, is the preparation of an ultra-fine microstructure (sub 100 nm range). And, another is the addition of catalytic elements like transition metals, rare-earth (RE) metals and transition metal oxides [2,3]. Different methods can be applied to produce so ultra-fine microstructure and catalyst containing Mg materials. Melt spinning, in particular, is very suitable to obtain high purity amorphous and/or nanocrystalline alloys with a very homogeneous microstructure at high production rate and low processing costs [4–6]. Also alloying magnesium with rare earth (RE) elements can improve the hydrogen absorption and desorption rates [7–10], and many studies have been conducted on Mg–Ni–La alloy [11–15]. The improvement of absorption kinetics can be ascribed to the nano-sized particles of rare earth metal hydrides and Mg₂Ni embedded in Mg matrix after activation, and the enhancement of desorption kinetics is attributed to the nano-sized particles of rare earth metal hydrides and Mg₂NiH₄ embedded in MgH₂ matrix after hydrogenation [16–19]. It is also well known that melt spinning technique is often employed [20–22] to lower the formation enthalpy of hydride for the high free volume of amorphous material [23,24].

In previous work, we have succeeded in preparing $Mg_{70}(Ni_3La)_{30}$ and $Mg_{70}(Ni_{3.5}La)_{30}$ by melt spinning to study the glass-forming kinetic properties of La-Mg-Ni alloys [25] and the hydrogen storage properties of $Mg_{70}(Ni_3La)_{30}$ alloy with different methods of melt spinning and as-melt [26]. The experimental results indicates that a three-dimensional interface reaction process of nucleation and growth for the initial hydrogenation kinetics and "geometrical contraction model" for dehydrogenation. Further more in this study, a series of experiments have been carried out to investigate the catalytic effect of rare earth metal (RE = La, Pr, Nd) on hydrogen absorption/desorption properties of as-prepared $Mg_{70}(RE_{25}Ni_{75})_{30}$ alloys, as well as the thermal stabilities of their hydrides.

^{*} Corresponding author. Tel.: +86 0773 2231906; fax: +86 0773 5601516. E-mail address: ghab1987@163.com (Z.-m. Wang).

2. Experimental

The intermediate alloys $RE_{25}Ni_{75}$ (RE = La, Pr, Nd) were prepared by arc melting of pure La, Pr, Nd and Ni (purity better than 99.9%). The master alloy $Mg_{70}(RE_{25}-Ni_{75})_{30}$ (RE = La, Pr, Nd) were prepared by induction melting with appropriate amounts of pure Mg and $RE_{25}Ni_{75}$ (RE = La, Pr, Nd). Then the $Mg_{70}(RE_{25}Ni_{75})_{30}$ (RE = La, Pr, Nd) alloys were quenched by melt-spinning with a constant rotating copper roller surface velocity of 20 m/s. About 5 wt.% of Mg were excessively added to compensate for the losses of Mg during melting and melt spinning.

To evaluate the phase structures of the melt-spun and hydrogenated samples, powder X-ray diffraction (XRD; Bruker D8 diffractometer; Cu K α radiation) measurements were carried out with a scan step of 5° /min. The hydrogen absorption/ desorption kinetics for the samples was measured under 2 MPa and vacuum using a Sieverts-type apparatus at 523 K, 553 K and 573 K respectively. P–C isotherms relationships were measured at 573 K, with a step of 0.03 MPa and 0.05 MPa for hydrogen absorption and desorption respectively. Prior to the measurements, the samples were fully activated by repeatedly hydriding at 573 K and dehydriding at 623 K for three times. In each activation cycle, the samples were first hydrogenated under a hydrogen pressure of 2 MPa for 10 h and then dehydrogenated under vacuum (10^{-3} Pa) evacuated for 1 h. Thermal properties of hydrogenated samples were investigated by differential scanning calorimetry (DSC, NET ZSCH STA 449F3) at different ramping rates (5, 10, 20, 30 K/min) under a continuous argon flow from 303 K to 873 K.

3. Results and discussion

3.1. Structural characterization

Fig. 1A shows the XRD patterns of the melt-spun Mg_{70} ($La_{25}Ni_{75}$)₃₀, $Mg_{70}(Pr_{25}Ni_{75})_{30}$, $Mg_{70}(Nd_{25}Ni_{75})_{30}$ alloys. It can be seen that all alloys prepared exhibit broad peaks at the position of about $2\theta = 30-45^{\circ}$, indicating the formation of fully amorphous phase. Similar results have been reported in Mg–Ni–RE alloys with excellent glass-forming ability [27,28].

The XRD patterns for the hydrogenated $Mg_{70}(RE_{25}Ni_{75})_{30}$ sample under a hydrogen pressure of 2 MPa at 573 K are shown in Fig. 1B. The rare earth metal hydrides $LaH_{3.01}$ (RE = La), $PrH_{2.92}$ (RE = La),

3.2. Hydrogen absorption/desorption kinetics

Fig. 2 shows the initial hydrogen absorption activation curves of $Mg_{70}(RE_{25}Ni_{75})_{30}$ alloys. It can be clearly seen that the initial hydrogen absorption activation process is quite slow. After activation, the hydrogen absorption/desorption kinetics properties of

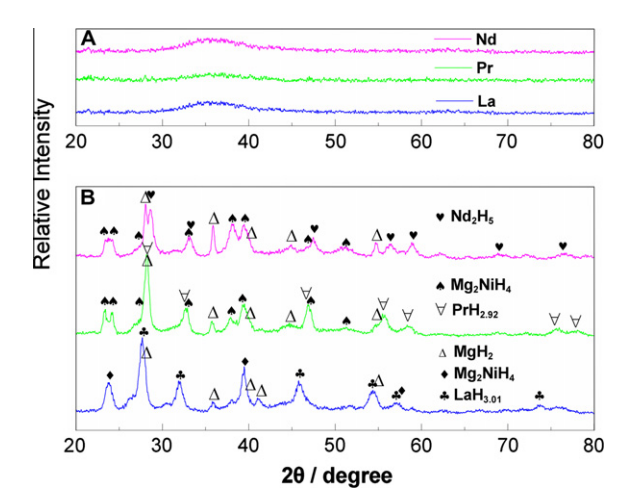


Fig. 1. The XRD patterns of $Mg_{70}(RE_{25}Ni_{75})_{30}$ alloys (a) melt-spun and (b) hydrogenated samples.

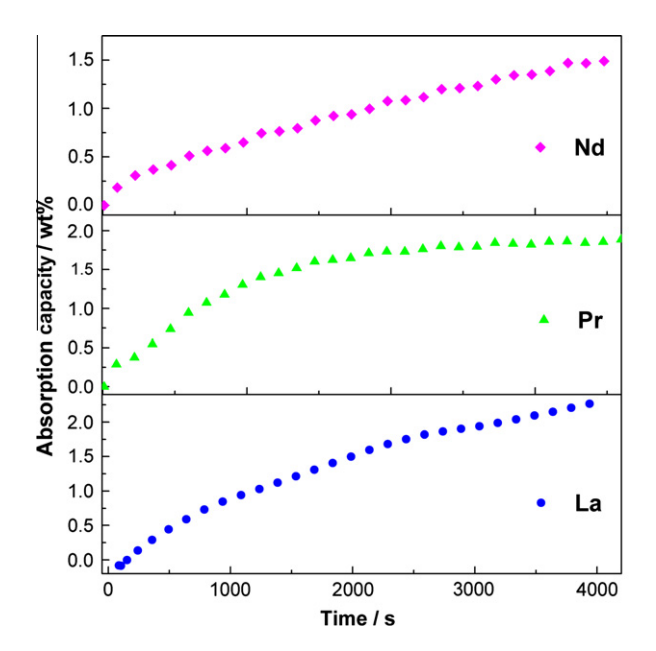


Fig. 2. Initial hydrogen absorption activation curves of Mg₇₀(RE₂₅Ni₇₅)₃₀ alloys.

Mg₇₀(RE₂₅Ni₇₅)₃₀ alloys were measured. Fig. 3 presents the kinetic curves of hydrogen absorption/desorption of the activated Mg₇₀(RE₂₅Ni₇₅)₃₀ alloys under an initial hydrogen pressure of 2 MPa/vacuum at 523 K, 553 K and 573 K, respectively. From Fig. 3a the first hydrogen absorption kinetics curve, the reaction rate (meaning the ratio of reacted material to the total hydride material) were more than 90% in 250 s, compared with Fig. 2 which implies that all the samples were fully activated. That is to say, three hydriding–dehydriding cycles at 573 K are sufficient to activate the melt-spun alloys. Such a result can be ascribed to the rare earth metal hydrides and Mg₂NiH₄ produced during the hydrogenation process. Moreover, the maximum hydrogen absorption/desorption capacity values are listed in Table 1.

It was noted that the reaction rate of the hydrogen absorption increases according to the subsequence Pr > La > Nd at 523 K in 250 s, while at 573 K the hydrogen absorption rate increase according to the subsequence Nd > Pr > La. The difference of maximum hydrogen absorption capacity between 523 K and 573 K were Nd > La > Pr in Table 1. This means that the catalytic effect change on the different rare-earth metal hydrides were Nd > La > Pr with the increase of temperature during the hydrogen absorption process. Also, Table 1 and Fig. 3 show that the hydrogen desorption kinetics were in the order of Pr > La > Nd and the maximum hydrogen desorption capacity was 2.79 wt.% for Mg₇₀(Pr₂₅Ni₇₅)₃₀ at 573 K. The maximum hydrogen capacity ratio of desorption to absorption was bigger with the increase of temperature and the supreme values was 92.38% at 573 K of $Mg_{70}(Pr_{25}Ni_{75})_{30}$ alloy. For the samples, indicate that the different rare earth metal hydrides catalytic effect was Pr > La > Nd at all the temperature during the hydrogen desorption process.

The hydriding mechanism has been further discussed by different reaction processes in previous Ref. [32–34], such as (1) chemical reaction (Eq. (1) with a differential form as Eq. (2)) [35], (2) nucleation and growth processes (Avrami–Erofeev equation [36–38], Eq. (3)), (3) autocatalytic reactions (Eq. (4)), (4) phase-boundary-controlled reactions, and (5) diffusion-controlled reactions.

$$a/(1-a) = k(t-c) \tag{1}$$

$$da/dt = K(1-a)^2 (2)$$

Download English Version:

https://daneshyari.com/en/article/1614170

Download Persian Version:

https://daneshyari.com/article/1614170

<u>Daneshyari.com</u>